Available online at www.sciencedirect.com
ScienceDirect
Ceramics International 35 (2009) 2469–2473
CERAMICS INTERNATIONAL
www.elsevier.com/locate/ceramint

Fabrication of porous magnesium spinel with directional pores by unidirectional solidification

S. Ueno [a,*], T. Akatsu [b], H. Nakajima [a]

[a] The Institute of Scientific and Industrial Research, Osaka University, 8-1 Mihogaoka, Ibaraki, Osaka 567-0047, Japan
[b] Materials and Structure Laboratory, Tokyo Institute of Technology, 4259, Nagatsuta, Midori-ku, Yokohama 226-8503, Japan

Received 3 December 2008; received in revised form 5 January 2009; accepted 12 February 2009
Available online 11 March 2009

Abstract

A porous magnesium spinel ($MgAl_2O_4$) with directional pores was fabricated by unidirectional solidification in pressurized argon and hydrogen mixed gases. Two different kinds of pores with large directional and small facet shape were formed in the solidified samples. The former pores were dominant in the porous structure. A small amount of free corundum phase was formed in the solidified porous spinel as a secondary phase by vaporization of MgO component during the solidification process. With increasing total gas pressure, the pore size of the solidified samples decreased while no change in the porosity. The porosity and pore size of the samples increased with increasing hydrogen partial pressure. The porosities of the samples fabricated under 10%H_2–90%Ar and 1%H_2–99%Ar mixed gases were 30 and 10%, respectively, and that under Ar atmosphere was very low, non-porous.

Keywords: Unidirectional solidification; Hydrogen solubility; Porous spinel

1. Introduction

Porous ceramics with excellent chemical stability at high temperatures are promising for filters in corrosive gas flow such as for integrated coal gasification combined cycle (IGCC) powder generation systems [1–3]. Spinel ($MgAl_2O_4$) ceramic with high thermal and chemical resistances at high temperatures is a candidate for the gas filters [3,4].

The pore sizes for the gas filter applications are requested to be controlled between 10 μm and several hundreds μm [1]. Many research groups have been proposed for the fabrication process of the porous ceramics with open pores. Zhang et al. [5] fabricated porous alumina with unidirectionally aligned continuous pores by sintering of cotton fibers coated with alumina. Isobe et al. [6] prepared porous alumina with oriented cylindrical pores by an extrusion method using fibers as pore formers. However, in these methods, it is difficult to control the porosity and pore size of the porous alumina widely due to the restriction of fiber diameters. The present authors have proposed a fabrication process of porous alumina with cylindrical pores by unidirectional solidification in pressurized hydrogen atmosphere [7]. In this method, the porosity and pore size can be controlled by hydrogen partial pressure and total pressure [7].

In this paper, porous spinel ceramics with cylindrical pores were fabricated by unidirectional solidification in pressurized argon–hydrogen mixed gas and the formation mechanism of the pores was discussed.

2. Experimental procedures

For the preparation of $MgAl_2O_4$ feed rod, high purity alumina (99.99% purity, Sumitomo Chemical Co. Ltd.) and magnesia (99.9% purity, Konoshima Chemical Co. Ltd.) powders were used as the starting materials. The powders with the stoichiometric ratio were mixed with a binder in water and the slurry was poured into a mold. After drying in air, calcination at 1200 °C for 2 h in air, the feed rod with 8 mm diameter and 150 mm length was obtained.

The solidification was carried out using optical floating zone apparatus in pressurized argon–hydrogen mixed gases atmo-

* Corresponding author at: Materials Science & Technology Research Center for Industrial Creation, The Institute of Scientific and Industrial Research, Osaka University, 8-1 Mihogaoka, Ibaraki, Osaka 567-0047, Japan.
Tel.: +81 6 6879 8437; fax: +81 6 6879 8439.
E-mail address: ueno23@sanken.osaka-u.ac.jp (S. Ueno).

0272-8842/$34.00
doi:10.1016/j.ceramint.2009.02.021

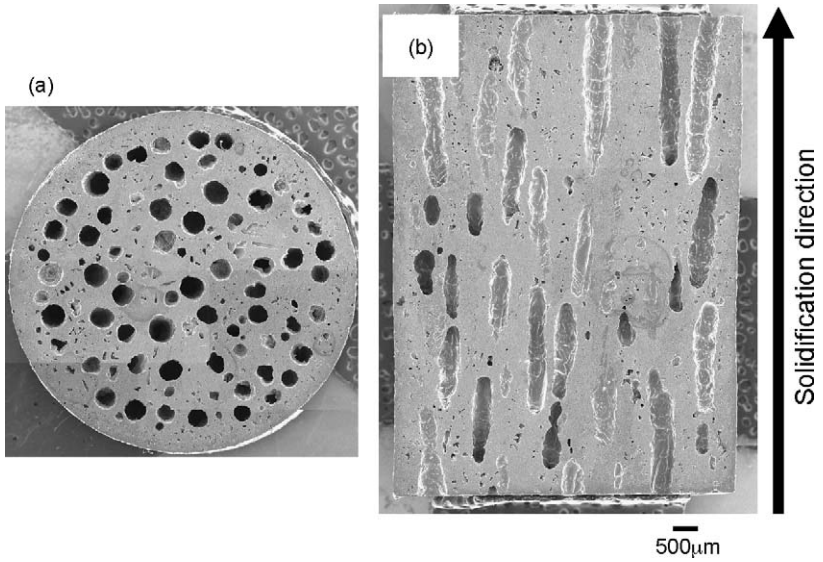

Fig. 1. Transversal (a) and longitudinal (b) cross-sections of a sample fabricated in 10%H_2–90%Ar mixed gas pressure of 0.4 MPa and a solidification rate of 300 mm/h.

sphere. Mixed gases with 10%H_2–90%Ar and 1%H_2–99%Ar were used in the experiments. The total gas pressure was controlled in the range from 0.1 to 0.7 MPa. Xenon lamp was used as a heating source. The xenon lamp and melting zone put on the focus in the elliptical mirror. A feed rod was hooked on the upper shaft and another feed rod was fixed at the lower shaft. This melting system was set up in a quartz tube. The atmosphere gas was introduced into the quartz tube. The transference velocity of the floating zone was controlled in the range from 100 to 400 mm/h.

The transversal and longitudinal cross-sections of the samples against the solidification direction were observed by an SEM (JEOL JSM-6360T). The porosity of the samples was calculated from the transversal cross-section images. From all pores in the cross-section, the area ratio was calculated for each pore. The porosity can be derived from the summation of the area ratio of pores.

The compressive strength test for the samples was performed according to JIS-R1608 using universal testing machine (Shimazu-200t Hydraulic System Universal Testing Machine). Cylindrical samples (approximately ϕ8 mm × 10 mm) were used for the test. The direction of the cylindrical pores was formed parallel to the stress loading direction. The compressive strength σ_c was calculated by the following equation

$$\sigma_c = \frac{4P}{\pi d^2} \quad (1)$$

where P and d are the ultimate load for crush and the diameter of the sample, respectively.

3. Results and discussion

Fig. 1(a) and (b) shows the transversal and longitudinal cross-sections of the sample fabricated in 10%H_2–90%Ar mixed gas pressure of 0.4 MPa and a solidification rate of 300 mm/h. Cylindrical pores are aligned in the solidification direction. In addition to the cylindrical pores, many small pores are also formed in whole of the sample. Porous samples with the same structure can be fabricated in pressurized 10%H_2–90%Ar and 1%H_2–99%Ar mixed gases. When 50%H_2–50%Ar mixed gas was used for the solidification, the inner wall of the quartz tube was quickly fogged up by the vaporized material and it was difficult to fabricate samples.

Fig. 2(a) and (b) shows the powder X-ray diffraction (XRD) patterns of the samples fabricated in 100%Ar and 10%H_2–90%Ar mixed gases at 0.4 MPa and solidification rate at 200 mm/h. All XRD peaks for (a) can be identified as $MgAl_2O_4$ phase. However, a small amount of Al_2O_3 phase can be detected in (b) as indicated by arrows. When the solidification is performed in 10%H_2–90%Ar and 1%H_2–99%Ar mixed gases, a vaporized material is deposited on inner wall of the quartz tube. Fig. 2(c) denotes the XRD pattern of the vaporized material. The strong peaks marked by circle can be indexed as MgO (ICDD card No. 87-0651) phase. However, some weak peaks can be also detected. The peaks marked by triangles may be identified as a solid solution of $(Mg,Al)(Al,Mg)_2O_4$ with spinel structure [8]. Some other unknown peaks were observed in the XRD pattern of (c). These results suggest that hydrogen gas accelerate the vaporization of MgO component.

Fig. 3 shows the transversal cross-section views of the samples fabricated in 1%H_2–99%Ar and 10%H_2–90%Ar mixed gases. Fig. 4 shows the porosity change as a function of the total pressure. If the pores are formed at the solid–liquid interface due to the difference of hydrogen solubilities of solid and liquid phases, the pressure of inner pore depends on the total pressure according to the following Eq. (2) and the volume of pores decreases with increasing total pressure according to the Boyle's law. Then, the porosity of the samples decreases with increasing total pressure

$$P = \frac{2\gamma}{R} + P_0 \quad (2)$$

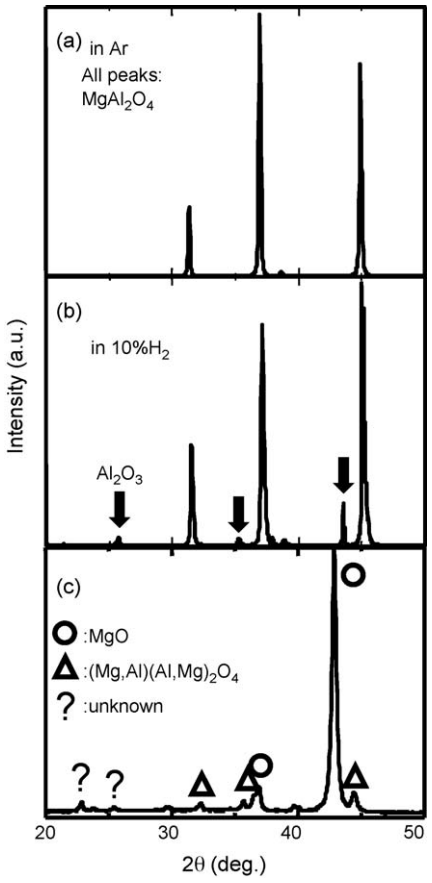

Fig. 2. The powder X-ray diffraction patterns of the samples fabricated (a) in 100%Ar and (b) in 10%H_2–90%Ar mixed gases at 0.4 MPa and solidification rate of 200 mm/h and that of the vaporized material (c).

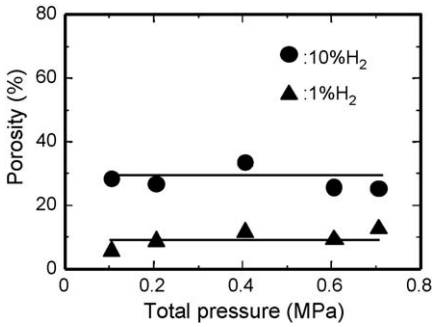

Fig. 4. The porosity change where, circle and triangular denote the porosity of the samples fabricated in 10%H_2–90%Ar atmosphere and in 1%H_2–99%Ar atmosphere.

where γ, R and P_0 are the surface tension of the liquid $MgAl_2O_4$ phase, pore radius and total pressure, respectively. However, the porosity did not change with total pressure. In the case of porous alumina by unidirectional solidification [7], the porosity decreased with increasing total gas pressure and increased with increasing hydrogen partial pressure. The pores are considered to be formed at the solid–liquid interface due to the difference of hydrogen solubilities of solid and liquid phases in this case. By contrast, another pore formation mechanism must be considered for the present samples.

Fig. 5(a) and (b) shows changes of the porosity and average pore diameter as a function of the total gas pressure; the porosity and pore size are evaluated using only large cylindrical pores. The porosity and pore size decrease with increasing total gas pressure and increase with increasing hydrogen partial pressure. When the cylindrical pores are formed at the solid–liquid interface due to hydrogen solubilities of solid and liquid phases, it is expected that the porosity increases with increasing

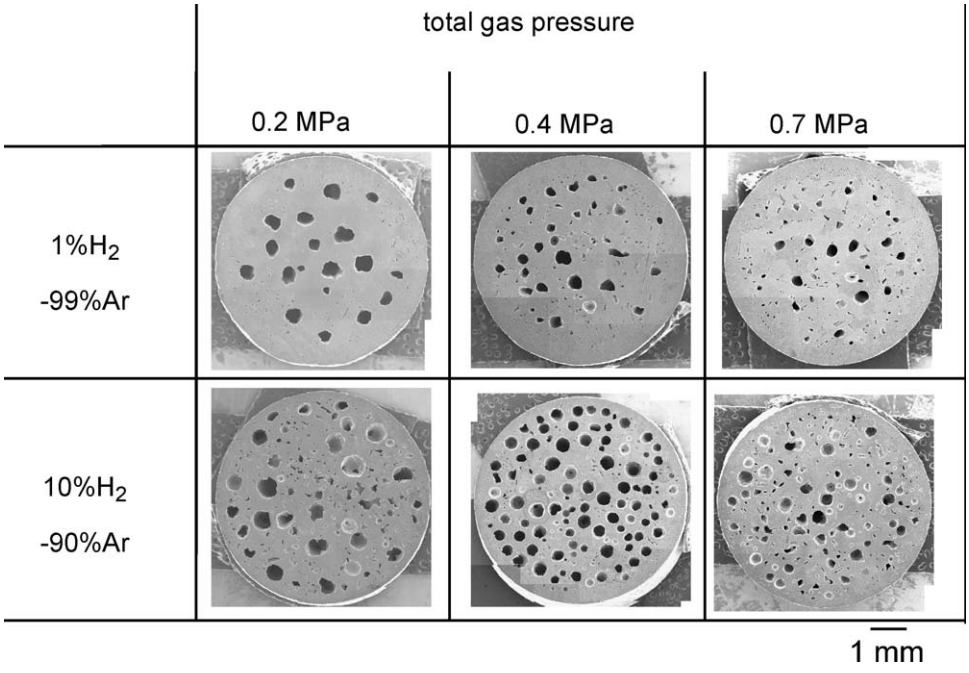

Fig. 3. The transversal cross-section view of the samples fabricated in 100%Ar and 10%H_2–90%Ar mixed gases.

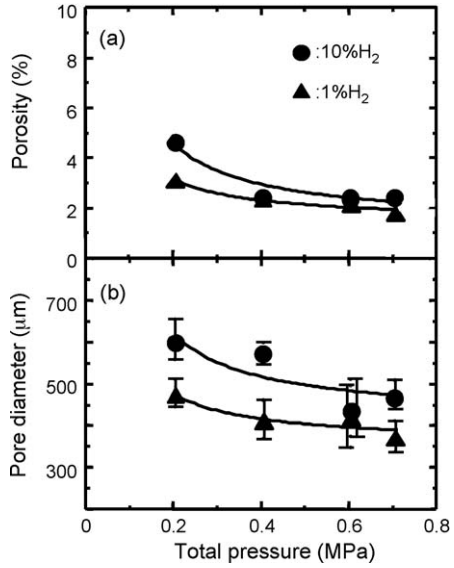

Fig. 5. The porosity (a) and average pore diameter (b) changes of the samples where the porosity and pore size are calculated using ten large pores in each sample those are cylindrical pores.

hydrogen partial pressure according to Sievert's law and decreases with increasing total gas pressure according to the Boyle's law as in the case of porous alumina [7]. The pore size also decreases with increasing total gas pressure according to the Boyle's law. Hence, it is confirmed that the cylindrical pores in the samples are formed at the solid–liquid interface due to the difference of hydrogen gas solubility in solid and liquid phases during the unidirectional solidification as in the case of porous alumina [7].

The small pores have a facet shape as indicated in Fig. 1. This suggests that the small pores are formed in a cooling step after the solidification. The porosity of the samples (Fig. 4) increases with increasing hydrogen partial pressure. Hence, the formation of the small pores is closely related to the hydrogen solubility in the solid phase. It is expected that the hydrogen solubility in solid $MgAl_2O_4$ phase also increases with increasing hydrogen partial pressure according to Sievert's law as in the case of alumina [12]. Hence, it is considered that the evaporation rate of MgO component from the solid phase below melting point is accelerated by the dissolved hydrogen in the solid phase and then, many small pores are formed in the bulk. The evaporation of MgO component from $MgAl_2O_4$ was reported by Altman [9] and Sasamoto et al. [10]. The Mg(g) partial pressure due to Eq. (3) is hundred times larger than that of Eq. (4) at high temperatures [9]

$$MgO(s) = Mg(g) + \tfrac{1}{2}O_2(g) \quad (3)$$

$$MgO(s) = MgO(g) \quad (4)$$

It can be understood the reduction reaction of Eq. (3) is accelerated by the dissolved hydrogen in the solid $MgAl_2O_4$ and the porosity increases with increasing the amount of dissolved hydrogen, namely, hydrogen partial pressure.

Fig. 6(a) and (b) shows the longitudinal cross-section views of the sample fabricated in 1%H_2–99%Ar at 0.4 MPa and

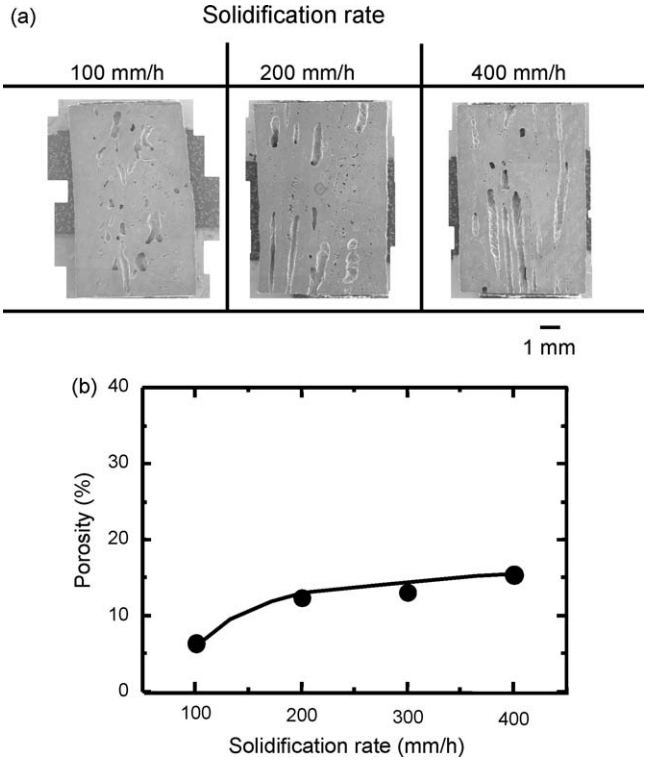

Fig. 6. The longitudinal cross-section view of the samples fabricated in 1%H_2–99%Ar of 0.4 MPa (a) and porosity change with solidification rate (b), where the porosity of the samples are calculated from the transversal cross-section.

porosity change with solidification rate, respectively. It can be seen that the porosity and length of the cylindrical pores slightly increases with increasing solidification rate. Thus, it is effective to control the porosity and morphology of the cylindrical pores by solidification rate.

The compressive strength of the samples fabricated in Ar and 10%H_2–90%Ar at 0.2 MPa are 619 ± 21 and 338 ± 41 MPa, respectively. The former sample is a non-porous bulk with a composition $MgAl_2O_4$ and the latter is a porous sample with 27.5% porosity with composition $MgAl_2O_4 + Al_2O_3$. It is known that the compressive strength of porous metals with cylindrical pores in pore direction σ is proportional to $\sigma_0(1-p)$, where p denotes the porosity [11]. The strength of the porous sample is slightly smaller than that of expected value 448 MPa. Since the porous sample has many small pores, it is considered that the lower strength from the expected value is attributed to the small facet shape pores.

4. Conclusion

A porous magnesium spinel with cylindrical pores and small facet shape pores can be fabricated by unidirectional solidification in pressurized Ar–H_2 mixed gas. The cylindrical pores are formed at the solid–liquid interface due to difference of the hydrogen solubilities between solid and liquid phase. On the other hand, small pores are formed by vaporization of MgO component from the solid $MgAl_2O_4$ in the cooling step after the solidification that is accelerated by dissolved hydrogen in solid $MgAl_2O_4$ phase. The compressive strength of the porous spinel

is slightly lower than that of expected value from the non-porous sample because of the existence of the small pores.

Acknowledgments

The present work was supported by Materials Science and Technology Research Center for Industrial Creation in Institute of Science and Industrial Research of Osaka University from the Ministry of Education, Culture, Sports, Science and Technology and the Grant-in-Aid for Scientific Research (C) (No. 18560655) by the Japan Society for the Promotion of Science. The compressive test was performed at Tokyo Institute of Technology on Collaborative Research Project of Materials and Structure Laboratory.

References

[1] R.W. Rice, Porosity of Ceramics, Marcel Decker, New York, 1998.
[2] M.A. Alvin, Impact of char and ash fines on porous ceramics filter life, Fuel Process. Technol. 56 (1998) 143–168.
[3] Y. Suzuki, N. Kondo, T. Ohji, Reactive synthesis of a calcium zirconate/spinel composite with idiomorphic spinel grains, J. Am. Ceram. Soc. 86 (2003) 1128–1131.
[4] Y. Suzuki, N. Kondo, T. Ohji, Uniformly porous composites with 3-D network structure (UPC-3D) for high temperature filter application, Int. J. Appl. Ceram. Technol. 1 (2004) 76–85.
[5] G.J. Zhang, J.F. Yang, T. Ohji, Fabrication of porous ceramics with unidirectionally aligned continuous pores, J. Am. Ceram. Soc. 84 (2001) 1395–1397.
[6] T. Isobe, T. Tomita, Y. Kameshima, A. Nakajima, K. Okada, Preparation and properties of porous alumina ceramics with oriented cylindrical pores produced by an extrusion method, J. Eur. Ceram. Soc. 26 (2006) 957–960.
[7] S. Ueno, L.M. Lin, H. Nakajima, Formation mechanism of porous alumina with oriented cylindrical pores fabricated by unidirectional solidification, J. Am. Ceram. Soc. 91 (2008) 223–226.
[8] R.C. Peterson, G.A. Lager, R.L. Hitterman, A time-of-flight neutron powder diffraction of $MgAl_2O_4$ at temperatures up to 1273 K, Am. Mineral. 76 (1991) 1455–1458.
[9] R.L. Altman, Vaporization of magnesium oxide and its reaction with alumina, J. Phys. Chem. 67 (1963) 366–369.
[10] T. Sasamoto, H. Hara, T. Sata, Mass-spectrometric study of the vaporization of magnesium oxide from magnesium aluminate spinel, Bull. Chem. Soc. Jpn. 54 (1981) 3327–3333.
[11] T. Ikeda, T. Aoki, H. Nakajima, Fabrication of lotus-type porous stainless steel by continuous zone melting technique and mechanical property, Metall. Mater. Trans. A 36A (2005) 77–86.
[12] E. Serra, A.C. Cosoli, L. Phillioni, Hydrogen permeation measurements on alumina, J. Am. Ceram. Soc. 88 (2005) 15–18.